Heliyon 5 (2019) e02112

Contents lists available at ScienceDirect

Heliyon

journal homepage: www.heliyon.com

Enhancing the mechanical properties of zirconia/Nafion® nanocomposite membrane through carbon nanotubes for fuel cell application

R. Sigwadi [a], M.S. Dhlamini [b], T. Mokrani [a], F. Nemavhola [c,*]

[a] Department of Chemical Engineering, University of South Africa, Private Bag X6, Florida, 1710, South Africa
[b] Department of Physics, University of South Africa, Private Bag X6, Florida, 1710, South Africa
[c] Department of Mechanical Engineering, University of South Africa, Private Bag X6, Florida, 1710, South Africa

ARTICLE INFO

Keywords:
Materials science
Nanocomposite
Water contact angle
Mechanical strength
Carbon nanotube
Impregnation

ABSTRACT

Membranes are widely used daily, such as for filtration in reverse osmosis, or in the form of electrolyte membrane fuel cells. Modified Nafion® membranes were synthesised by impregnation and their mechanical properties were observed. The effect of the incorporation of a ZrO_2-CNT nano-filler within Nafion® membrane on the thermal stability and crystallinity was investigated by TGA and XRD. Tensile test results show the increases in the mechanical properties of Nafion® 117 membranes impregnated with ZrO_2-CNT when compared with that of commercial Nafion® 117 membranes. The results also show that adding ZrO_2-CNT in Nafion® 117 membranes improves the water contact angle and water uptake, as it enhances water retention within the membrane. The SEM results indicated that ZrO_2-CNT was well distributed in the Nafion® 117 membrane pores through the impregnation method.

1. Introduction

Membranes are widely used daily, such as for filtration in reverse osmosis or in the form of electrolyte membrane fuel cells. However, many of them face mechanical and thermal failure under some operational conditions. Some of them can burn, shrink and fail structurally as a result of cracking, tearing, perforations and pinholes while functioning at low relative humidity and high temperatures due to internal defects. Therefore, it is necessary to improve their thermal stability, and mechanical and chemical strength in order to make them suitable for use in various conditions. The polymer electrolyte membrane fuel cells (PEMFCs) have been considered as environmentally friendly due to their zero emissions [1]. The performance of proton exchange membranes (PEMs) is highly dependent on their water content [1]. However, Nafion® membranes as state-of-the-art PEMs have a high chemical and mechanical stability, high proton conductivity at a lower temperature of 80 °C and high relative humidity. But, it faces some drawbacks when operating at a higher temperature fuel cell, as it lowers proton conductivity due to the membrane dehydrating [2]. The incorporation of inorganic particles such as silica, titanium and zirconium nanoparticles has been found to improve the thermal and mechanical stability and enhance water retention of commercial Nafion® 117 membranes at high temperatures and low relative humidity [3]. Because of strong covalent bonds that limit dislocation slip and therefore plastic deformation in comparison with metallic materials [4, 5], modified membranes with zirconium oxide nanoparticles can be used in many applications such as solid oxide fuel cells, oxygen sensors and ceramic membranes due to their good high-temperature stability, high breakdown electrical field or large energy bandgap [6]. However, with increasing temperatures, other thermally activated mechanisms such as grain boundary sliding [4] accommodated by diffusional creep lead to time-dependent plastic or even superplastic deformation composites [4]. Furthermore, the inorganic particles also play an important role in the field of dielectric and electrical applications [7]. Zirconium oxide nanoparticles (ZrO_2) is very important in ceramic materials because of their excellent electrical, thermal and mechanical properties [8]. ZrO_2 are the most intensively studied materials owing to their technologically important applications in oxygen sensors, fuel cell electrolysis, catalyst and catalytic supports, metal oxide semiconductor devices, and superior thermal and chemical stability [9]. This is due to their high melting point, high mechanical properties, low thermal conductivity and high ionic conductivity. The high temperature phases cubic (c-) and tetragonal (t) of ZrO_2 can be achieved at the lower synthesis temperature, which could be used as reinforcement for toughening aluminium as they are phase-transformation, phase-conversion and micro-cracking [10]. Much attention was being paid to controlling the morphology of ZrO_2 at the

* Corresponding author.
E-mail address: masitfj@unisa.ac.za (F. Nemavhola).

https://doi.org/10.1016/j.heliyon.2019.e02112
Received 14 January 2019; Received in revised form 11 June 2019; Accepted 16 July 2019

Fig. 1. Tensile mechanical testing of zirconia/Nafion® nanocomposite membrane (a) Clamp; (b) specimen - pure Nafion® membrane and Nafion®/ZrO_2 nanocomposite membrane.

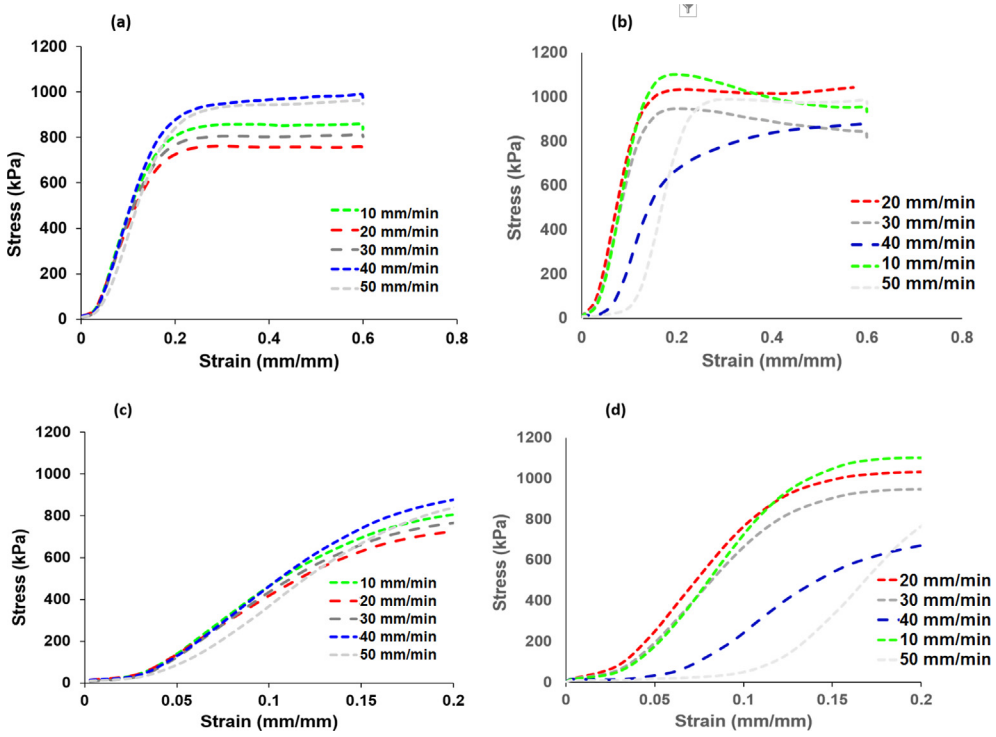

Fig. 2. (a) Nafion®/ZrO_2-CNT stress versus strain, (b) Nafion® 117 stress versus strain, (c) Low strain of Nafion®/ZrO_2-CNT nanocomposite membrane and (d) Low strain of Nafion® 117 membrane.

nanoscale for potential applications in gas sensors, catalyst and drug delivery [11]. Carbon nanotubes (CNTs) have good mechanical properties, are low-cost material and have high electrical conductivity with high surface area [12, 13, 14]. CNTs as inorganic fillers show the mechanical and thermal improvement, as well as a low electrical percolation threshold by producing a bridging effect when the ceramics are subjected to a tensile load, which results in enhancing its fracture toughness [15, 16]. Moreover, CNTs composited with metal oxides show improvement in the electrochemical energy system [17, 18]. They also have the ability to decrease equivalent series resistance (ERS), leading to an improved maximum power in super capacitors [19, 20]. CNTs could also enhance the tri-biological behaviour of ceramics, as the CNTs are relatively hard

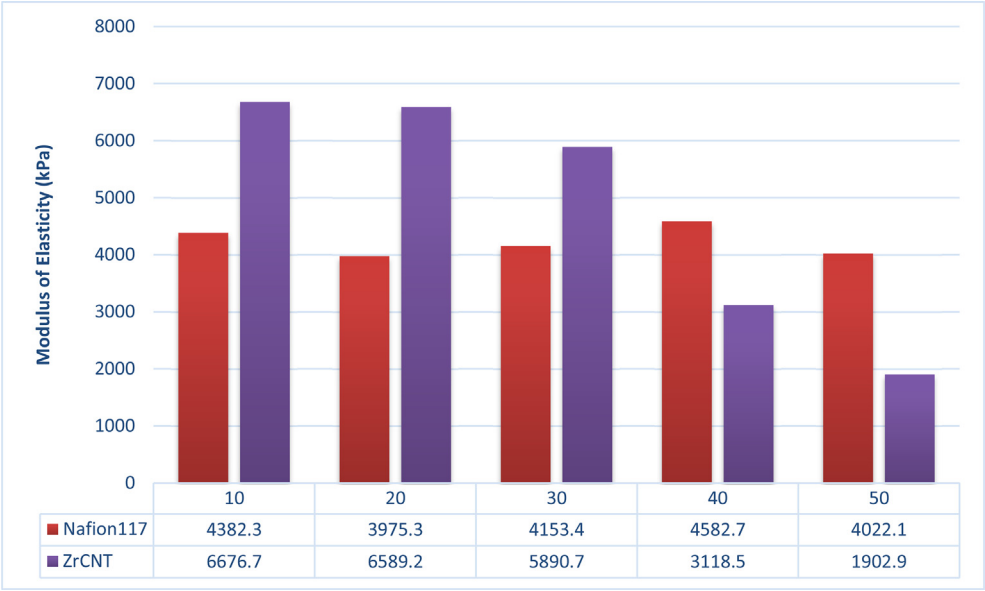

Fig. 3. Comparison of modulus of elasticity of Nafion® 117 membrane and Nafion®/ZrO_2-CNT nanocomposite membrane.

materials. If membranes are modified with carbon nanotubes (CNTs) their thermal stability, flame redundancy and electrical properties increase [21, 22]. The results suggested that it would be possible to toughen the membrane and enhance the water retention by adding ZrO_2-CNT to the nanometre zirconia particles. The aim of this paper is to investigate the influence the addition of ZrO_2-CNT has on the mechanical and physical structure of commercial Nafion® 117 membrane. ZrO_2 nanoparticles were composited with CNTs in order to increase the mechanical and chemical strength and thermal stability of commercial Nafion® 117 membrane. The influences of stress-strain on the mechanical strength of Nafion® 117 and modified Nafion® membrane were observed under 10 mm/min, 20 mm/min, 30 mm/min, 40 mm/min and 50 mm/min.

2. Experimental

2.1. Reagents

Zirconium oxychloride hydrate ($ZrOCl_2$.$8H_2O$), sodium hydroxide pellets (NaOH), hydrogen peroxide, methanol solution, sulphuric acid, carbon nanotubes (CNTs), nitric acid and Nafion® 117 membranes (EW = 1100, thickness 180) were purchased from Sigma. All the chemicals with analytical grade were used as received, without any further purification.

2.2. Preparation of ZrO_2-CNT nanocomposite

The zirconium oxide (ZrO_2) nanoparticles were prepared by the precipitate method; zirconium oxychloride hydrates ($ZrOCl_2.8H_2O$) and sodium hydroxide (NaOH) were used as starting materials. Precipitation of zirconium hydroxide ($Zr(OH)_4$) was obtained by slowly adding 2N NaOH to the aqueous solution of 0.2M $ZrOCl_2.8H_2O$ at room temperature while continuously stirring with a magnetic stirrer and mixed for 30 minutes [23]. The CNTs used for templating were synthesised by the aerosol-assisted CVD method [24]. The obtained CNTs were functionalised by refluxing in nitric acid and then washed to remove the excess acid. The purified CNTs were dispersed in a zirconia solution by the reflux method for two hours at 80 °C. The obtained products were centrifuged and washed with distilled water until the pH was neutral. Then it was dried at 80 °C overnight and calcinated at 600 °C for one hour [24].

2.3. Preparation of nanocomposite membrane

Nafion® 117 membranes were treated according to the standard procedure one hour in a boiling 3% solution of hydrogen peroxide; one hour in boiling 0.5 M sulphuric acid; one hour in boiling distilled water [25]. The nanocomposite membranes were prepared by soaking the Nafion® 117 membrane in the methanol solution in order to open the pores of membrane and followed by adding the required amount of ZrO_2-CNT (5 wt %) nanoparticles in a methanol solution. The nanocomposite membranes were repeatedly impregnated (up to five times) at room temperature [26]. The air from the nanocomposite membrane pores was removed by heating the solution for 2 hours up to 100 °C, then slowly cooled down to room temperature and kept in solution for further 24 hours. After drying, thicknesses of the nanocomposite membranes were measured with digital micrometre (0.18 mm). Each thickness was measured in the average of 3–7 reading at different position of membrane and was repeated twice on each membrane to obtain the average value.

2.3.1. Characterisation of nanocomposite membranes

The changes in the chemical structure of the membranes were investigated by Fourier Transform Infrared (FTIR). The crystallinity of the modified membranes was investigated by X-ray diffraction (XRD). The surface morphology of the membranes was analysed by atomic force microscopy (AFM) and scanning electron microscopy (SEM). The thermal behaviour of the membranes was investigated by thermo-gravimetric analysis (TGA).

2.3.2. Tensile testing

Tensile tests were conducted on modified membrane and commercial membrane by using a uniaxial testing system. The uniaxial mechanical properties of membrane were captured using a uniaxial testing system as shown in Fig. 1. The length, width and thickness of samples were measured using a Vernier caliper and recorded prior to testing. The testing area of the membrane sample was 4 mm × 10 mm in dimension. To allow for a clamping area, the sample was prepared in such a way that it could be clamped both side and still allow the testing area to be 4 mm × 10 mm. The thickness of the membrane was measured to be 0.18 mm. The thickness of 0.18 mm of the modified membrane and commercial membrane was used in analysing the stress applied to the sample. The membrane was soaked in water for 24 hours, and tested as a wet test. Then the membrane was dried in a vacuum oven at 80 °C for 24 hours

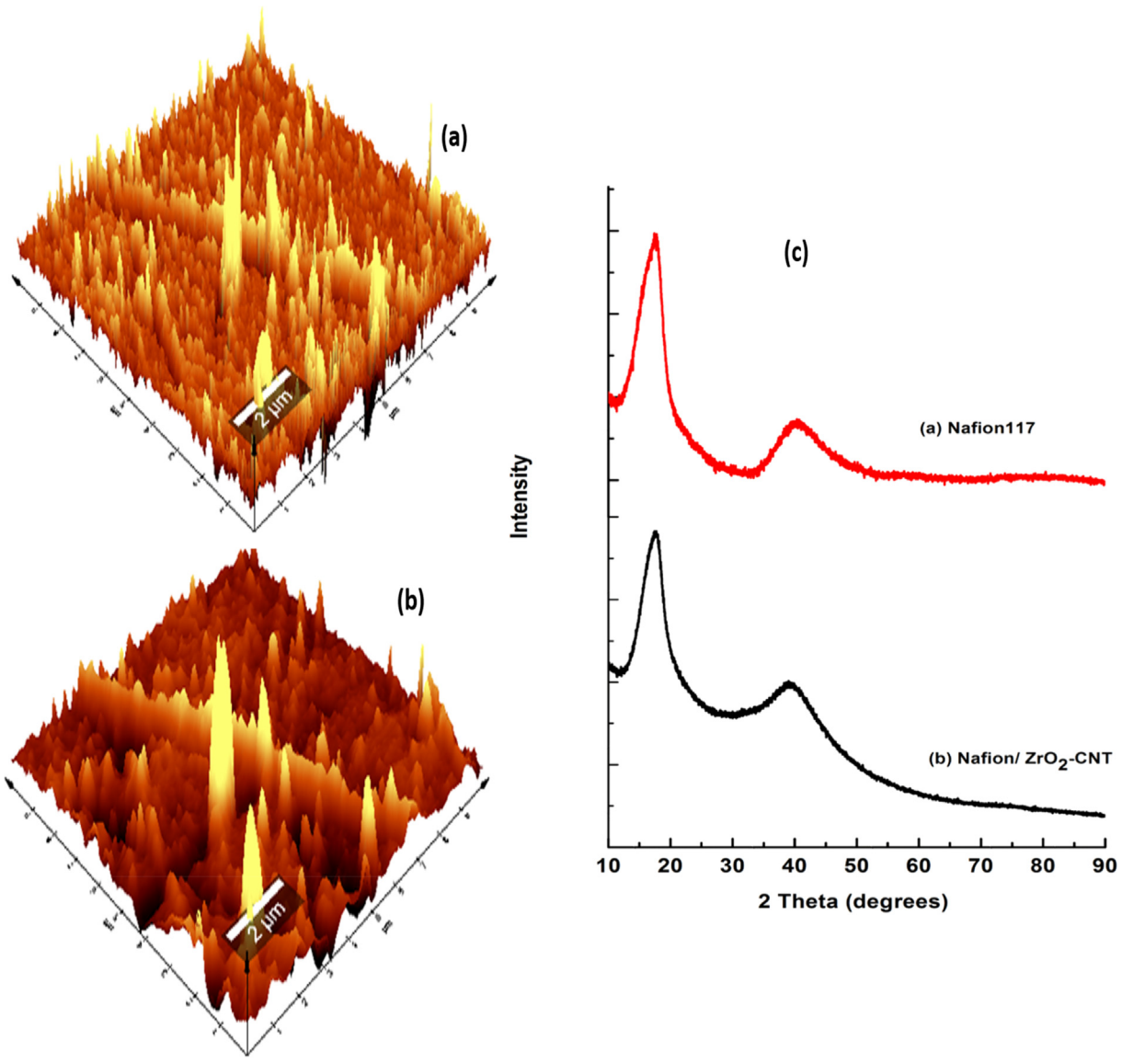

Fig. 4. Atomic force microscopy (AFM) (a) amplitude (b) topographies measured in tapping mode of the Nafion®/ZrO_2-CNT nanocomposite membrane and (c) The comparison of the XRD patterns of the (a) Nafion® 117 membrane and (b) Nafion®/ZrO_2-CNT nanocomposite membrane.

and tested as a dry test. The tensile strength of modified Nafion® membranes was measured using CellScale Ustretch device dried at 25 °C and actuator speed of 10 mm/min, 20 mm/min, 30 mm/min, 40 mm/min, 50 mm/min [27].

2.3.3. Contact angle measurements

The hydrophilicity of the membrane surfaces was performed under a contact angles measurement instrument equipped with a video system. Membranes were cut into strips and mounted on glass slides for analysis. The droplet of de-ionized water (2 μL) was dropped onto the surface of the membranes at ambient temperature by placing the tip of the syringe close to the sample surface, with all the images being captured on camera. The measurement was repeated 10 times at different surfaces of the membrane to obtain an average value. Before the water droplet attached to the sample surface, the wetting process was recorded until no significant change at the surface was observed any more. Then the contact angle was measured at different times during the wetting process. In this way, time-dependent contact angles were obtained [28].

2.3.4. Water uptake (Wup %) and swelling ratio (SR)

The membranes were soaked in distilled water for one day. They were then removed from the water, wiped, measured and weighed. Water uptake and swelling ratios were calculated according to the equations below:

$$W_{up}(\%) = \frac{(m_{wet} - m_{dry})}{m_{dry}} \times 100 \quad (1)$$

$$SR(\%) = \frac{(L_w - L_d)}{L_d} \times 100 \quad (2)$$

Where W_{up} is the percentage of water uptake, m_{wet} is the weight of wet membrane and m_{dry} is the weight of the dried membrane, L_w is the length of the wet membrane and L_d is the length of the dried membranes.

2.3.5. Ion exchange capacity

The ion exchange capacity (IEC) of all membranes were determined by the titration method. The titrated IEC of the membranes were determined by:

$$IEC = \frac{V_{NaOH} \ X \ C_{NaOH}}{W_{sample}} \quad (3)$$

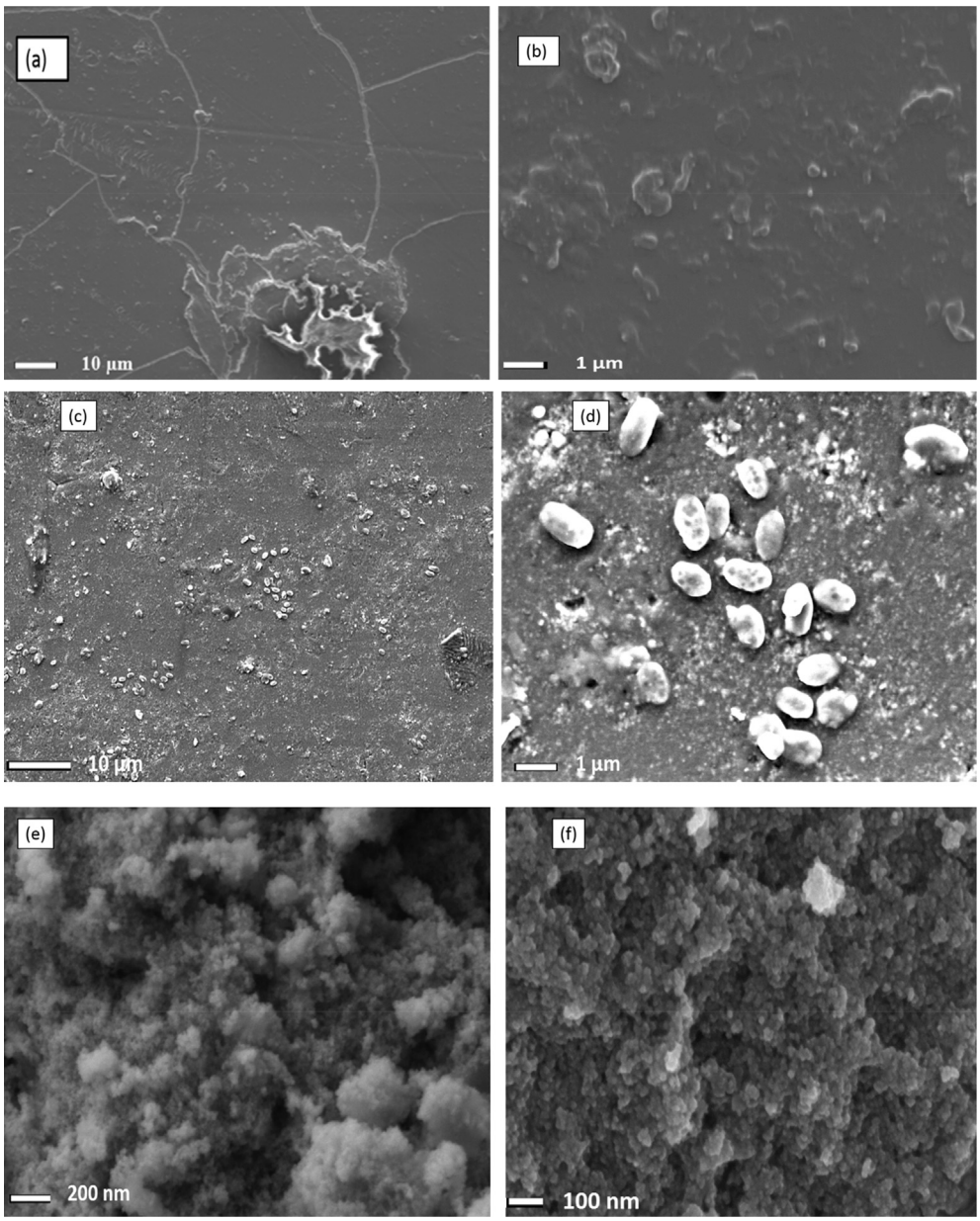

Fig. 5. SEM structures of (a-b) Nafion® 117 membrane, (c-d) Nafion®/ZrO_2-CNT nanocomposite membrane and (e-f) ZrO_2-CNT nanoparticles.

where V_{NaOH} is the titrated volume of NaOH and W_{sample} is the weight of the dry membranes.

2.3.6. *Conductivity measurement*

The conductivities of all membranes were measured using a four-point probe conductivity cell. The ionic conductivity was determined galvanostatically with a current amplitude of 0.1 mA over frequencies ranging from 1MHz to 10Hz. Using a Bode plot, the frequency region over which the impedance had a constant value was checked and the electrical resistance was then obtained from a Nyquist plot [29]. The ionic conductivity (σ) was calculated according to the following equation:

$$\sigma = L/RWd \quad (4)$$

where R is the obtained membrane resistance, L is the distance between potential-sensing electrodes (1 cm), and W and d are the width (2 cm) and thickness of the membrane (0.0183cm). For conductivity testing, the membrane was immersed in 1M sulfuric acid solution for six hours at room temperature. The membrane was then rinsed with deionised water several times to remove any excess H_2SO_4 then immersed in deionised water for six hours at 60 °C. All the membranes were kept in deionised water at room temperature before measurement.

3. Results

3.1. *Mechanical properties of membranes*

The tensile test was used to observe the mechanical strengths of the nanocomposite membranes compared with commercial Nafion® 117 membranes [30]. The results show that the incorporation of a ZrO_2-CNT nano-filler within the Nafion® membrane enhances the elasticity of a membrane at the strain rate of 10 mm/min, 20 mm/min, 30 mm/min, 40 mm/min and 50 mm/min as presented in Fig. 2(a and c). The results revealed that the stress-strain of Nafion®/ZrO_2-CNT nanocomposite membranes shows more improvement at the strain rate of 20 mm/min compared to that of the commercial Nafion® 117 membranes as shown in Fig. 2(a-b). The stress-strain of Nafion®/ZrO_2-CNT at the low strain of

(a)

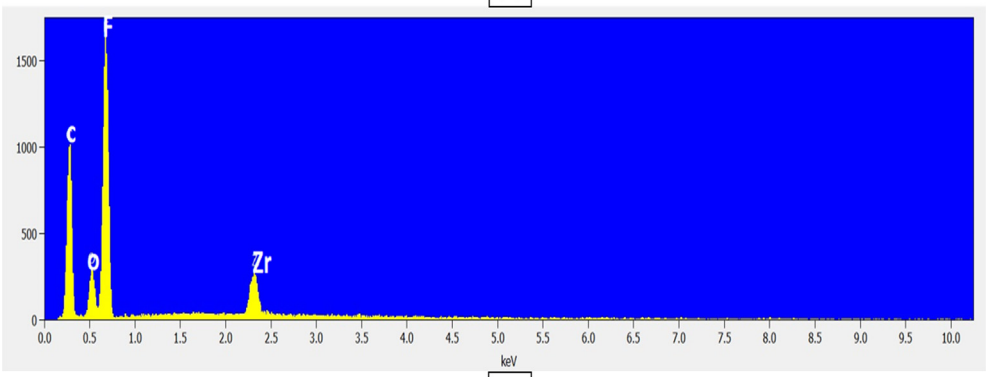

(b)

Element Line	Element Wt.%	Norm. Wt.%	Atom %	Compnd Formula	Compnd Wt.%	Norm. Compnd
C K	45.3	45.3	56.7	C	45.3	45.3
O K	8.5	8.5	8.0	O	8.5	8.5
F K	42.6	42.6	33.7	F	42.6	42.6
Zr L	3.5	3.5	1.7	Zr	3.5	3.5
Total	100.0	100.0	100.0		100.0	100.0

Fig. 6. (a) EDAX and (b) the elements of Nafion®/ZrO_2-CNT nanocomposite membrane.

0.17 was 1094 kPa, 1022 kPa, 938 kPa, 617 kPa and 550 kPa respectively, which is more of an improvement than those of Nafion® 117 membrane (753 kPa, 677 kPa, 714 kPa, 808 kPa and 753 kPa) as shown in Fig. 2(c-d). The modulus of elasticity of the Nafion®/ZrO_2-CNT nanocomposite membrane was higher than commercial Nafion® 117 membrane at the rate of 10 mm/min, 20 mm/min, 30 mm/min, 40 mm/min and 50 mm/min as shown in Fig. 3. This may be due to the addition of ZrO_2-CNT nanoparticles that causes the interaction with the sulfonic acid groups of the membrane, which enhanced the mechanical strength. Moreover, this enhanced modulus of elasticity shows that the ZrO_2-CNT nanoparticles have stabilised the structure of the nanocomposite membrane successfully, and give a potential restriction to the humidity-generated stress when the membrane is used as an electrolyte membrane in the fuel cells. Fig. 3 shows that the modulus of elasticity of the nanocomposite membrane at the small strain rate of 10 mm/min, 20 mm/min and 30 mm/min, increased the stress to 6677 kPa, 6589 kPa and 5891 kPa when compared to the 4382 kPa, 3975 kPa and 4153 kPa of commercial Nafion® 117 membrane. Furthermore, the modulus of elasticity of nanocomposite membranes decreases as the rates increase. At the higher rate of 40 mm/min and 50 mm/min ZrO_2-CNT nanoparticles become more rigid, which weakens the ionic interactions and change the mechanical stability.

3.2. Structures, morphology and elemental analysis of membranes

The amplitude and topography images measured in tapping mode of Nafion®/ZrO_2-CNT nanocomposite membranes was shown in Fig. 4. The modified membranes show that the presence of ZrO_2-CNT nanoparticles in the surface of Nafion® membrane shows the roughness of 12.79 nm. From the topography and amplitude images, we can clearly see no changes in the surface morphology, which indicates the strong interaction of filler material within the Nafion® matrix as shown in Fig. 4(a) and (b). More roughness on modified Nafion® nanocomposite membranes improves the contact between the electrodes [31]. The modified membranes show the presence of ZrO_2-CNT in the surface of membrane, which can be assigned to the hydrophobic (light regions)/hydrophilic (dark regions) domains across the membrane matrix due to the interaction of the sulphonic groups dispersed within the hydrophobic network of the Nafion® polymeric backbone [32]. The size of the light areas matches those observed for similar samples in the literature [33]. The crystallinity and morphology of nanocomposite membranes were analysed by X-ray diffraction (XRD) as shown in Fig. 4(c). Fig. 4(c) shows the XRD patterns of modified Nafion® membrane compared with commercial Nafion® 117 membrane. The results show the two broad diffraction peaks at 17° and 38° that assign to the amorphous and crystallinity scattering from the main chain of Nafion® 117 membrane as presented in Fig. 4c (a) [34, 35]. Fig. 4c (b) reflects the same peak as ZrO_2-CNT nanoparticles. Fig. 5 shows the morphological structures of nanocomposite membranes, commercial Nafion® 117 membrane and ZrO_2-CNT nanoparticles observed under SEM. Fig. 5(a-b) shows the original morphology of Nafion® 117 membrane with a dark colour when compared to the modified membrane. The ZrO_2-CNT nanoparticles in Fig. 5(c-d) were well distributed within the membrane, confirming the TGA results that show that the modified membrane is thermally more stable than Nafion® 117. This may be due to the inorganic filler distribution in the membrane [36] with less agglomoraton. Fig. 5(e-f) shows the ZrO_2-CNT nanoparticles agglomerated to each other with a diameter ranges from 5-10 nm. Fig. 6 shows the elemental composition of Nafion®/ZrO_2-CNT nanocomposite membrane under EDAX spectra. The nanocomposite membrane shows the present of carbon, oxygen, fluorine and zirconia as shown in Fig. 6(a). Furthermore, the elements table in Fig. 6(b) shows that ZrO_2-CNT nanoparticles were successfully impregnated within the Nafion® 117 membrane.

3.3. Degradation at high temperature

Thermo-gravimetric analysis (TGA)/derivative thermogravimetry (DTG) were used to determine the thermal stability of modified membranes and the commercial Nafion® 117 membranes. Fig. 7 shows the TGA and the derivative weight loss for Nafion® 117 membranes

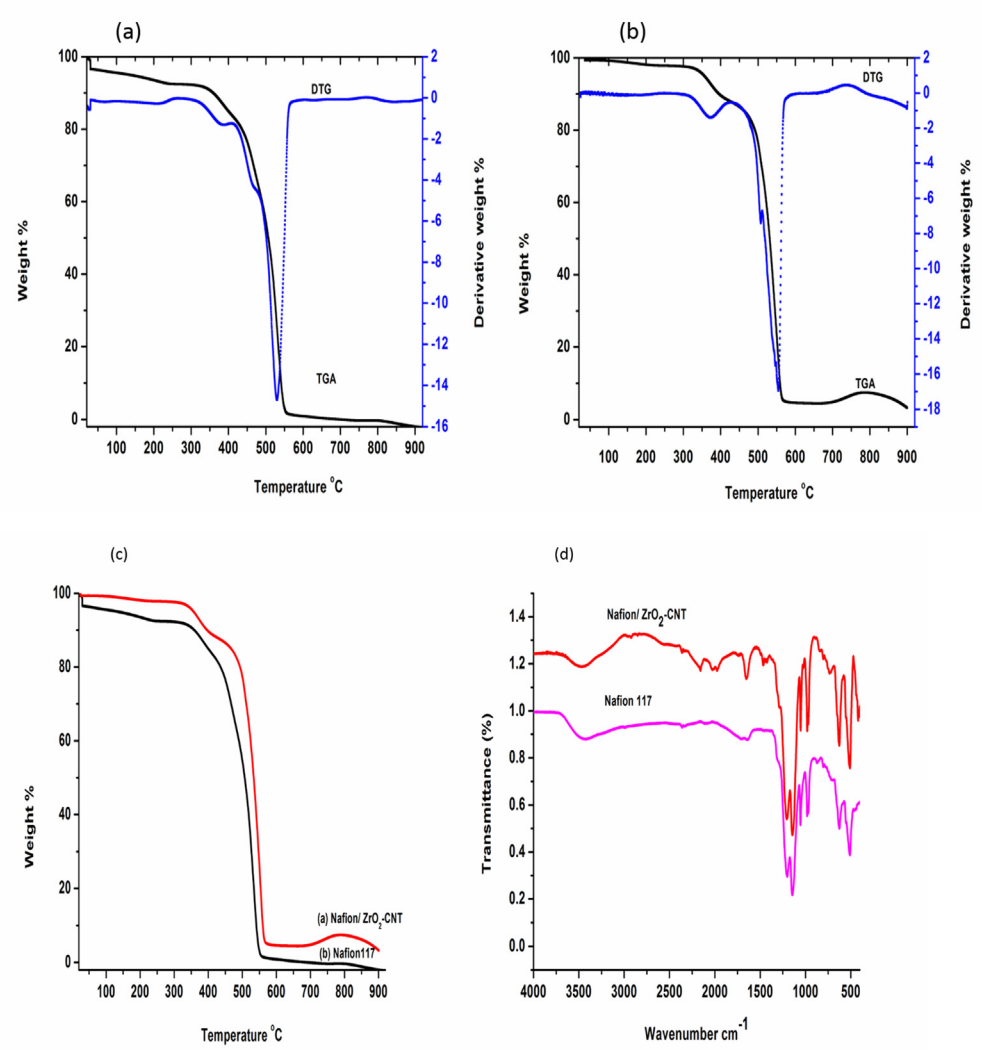

Fig. 7. The comparison of the TGA/DTG patterns of the (a) Nafion® 117 membrane, (b) Nafion®/ZrO_2-CNT nanocomposite membrane and (c) The comparison of the TGA patterns of (a) Nafion® 117 membrane and (b) Nafion®/ZrO_2-CNT nanocomposite membrane and (d) FTIR spectra of the (a) Nafion/ZrO_2-CNT nanocomposite membrane and (b) Nafion® 117 membrane.

compared with Nafion®/ZrO_2-CNT nanocomposite membranes. The results show that all membranes undergo three weight-loss stages. Fig. 7(a) shows the first decomposition stages at 390 °C with a gradual weight loss of 10%. This was attributed to water leaving the membrane. The second decomposition stages at 480 °C show a 38% weight loss, due to the desulfonation. The third decomposition stages at 550 °C show a 99.8% weight loss, due to the decomposition of the polymer backbone [37]. The TGA curves for commercial Nafion® 117 membranes show that the membrane was completely burnt as indicated in Fig. 7(a). The DTG curves show a maximum decomposition rate of 2% per °C at 390 °C and the weight loss in this step is 18%. The TGA curves of Nafion®/ZrO_2-CNT nanocomposite membranes also show three weight-loss stages. The first weight loss is at and 390 °C, which is attributable to water evaporating from the membrane. The second decomposition stage at 480 °C shows a 20% weight loss, due to the desulfonation process, and the third decomposition at 570 °C shows a 95.5% weight loss, due to the decomposition of the polymer backbone [37]. This indicated that the metal oxide was successfully deposited within the membrane through impregnation. Furthermore, modified membranes show less decomposition of sulfonic acid groups when compared with that of commercial Nafion® 117 membranes. The DTG curve shows the maximum decomposition rate of 2% per °C at 280 °C with a weight loss of 30%. TGA curves show that Nafion®/ZrO_2-CNT nanocomposite membranes have better thermal properties than commercial Nafion® membranes, as can be seen in Fig. 7(c). TGA analysis shows that the modified Nafion® 117 membrane was not subject to serious damage by the presence of ZrO_2-CNT until 500 °C, due to the reduced weight loss rate at a high temperature. Incorporating ZrO_2-CNT nanoparticles in Nafion® matrix leads to an increase in the decomposition temperature of nanocomposite membranes compared with commercial Nafion® 117 membranes. Thus, the result obtained from TGA shows the enhanced potential of the Nafion®/ZrO_2-CNT nanocomposite membranes for higher-temperature operations for PEMFC applications.

The degradation of the nanocomposite membranes compared with commercial Nafion® 117 membranes was investigated by FTIR as shown in Fig. 7(d). Fig. 7d(a) shows that vibration bands at 863 cm^{-1} and 926 cm^{-1} are due to the Zr–O vibration [38] and the peak at 1393 cm^{-1} and 1434 cm^{-1} are assigned to O–H bonding [38]. The peak observed at 2 346 cm^{-1} is due to the presence of inorganic ions [39]. The weaker band near 1055 cm^{-1} originates from the symmetric stretching of SO_3^- groups. The doublet peaks at 970 cm^{-1} and 982 cm^{-1} are characteristic peaks of the side chains of Nafion®, and are due to the symmetric vibrations of Zr–O bonds. The strong absorption bands near 1151 cm^{-1} and 1214 cm^{-1} are attributed to the symmetric stretching of -CF_2 groups and a mixed contribution from the anti-symmetric stretching modes of -CF_2 and -SO_3^- groups [40]. Fig. 7d(a) shows that the FTIR spectra of Nafion®/ZrO_2-CNT

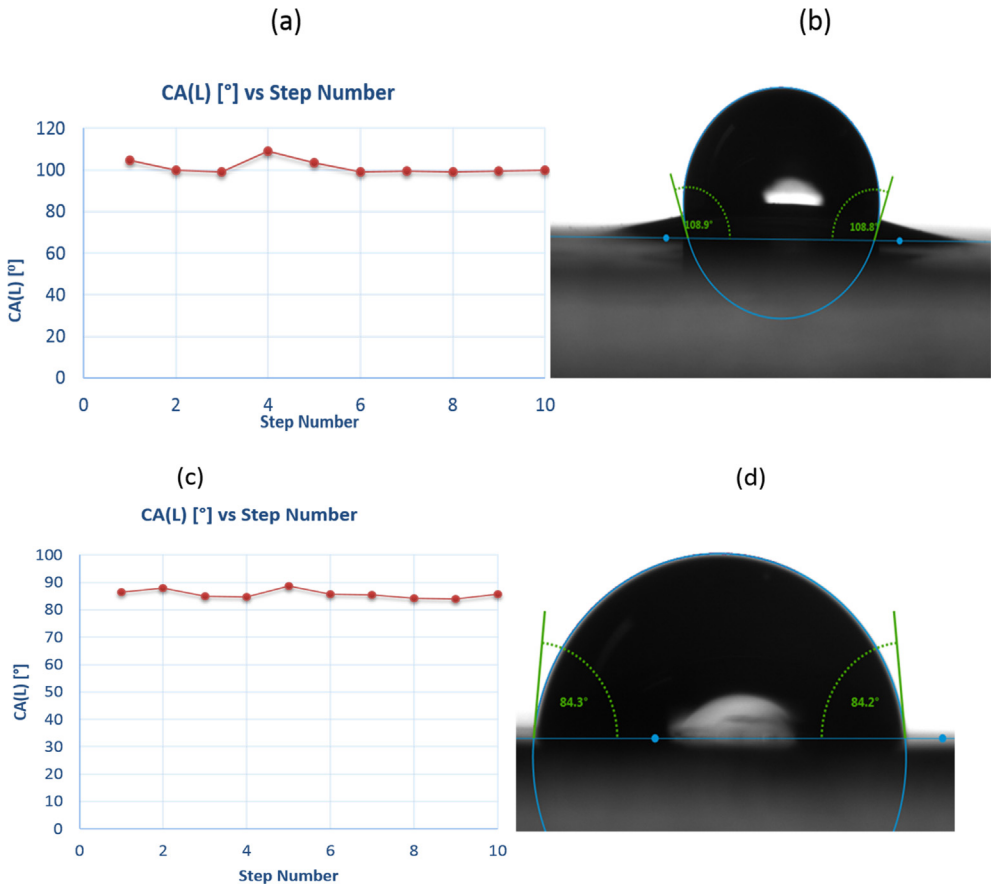

Fig. 8. The water contact angle of (a-b) Nafion 117 membranes and (c-d) Nafion/ZrO_2-CNT nanocomposite membrane.

Table 1
The The IEC, water uptake, swelling ratio and conductivity of membranes.

Membrane	IEC (meq. g^{-1})	Water Uptake	Swelling Ratio	Conductivity (S/cm)
Nafion®/ZrO_2-CNT	1.36	52	16.7	0.265
Nafion® 117	0.93	30	8.8	0.113

indicate some peaks due to the grafted amine groups. The N–H stretching vibrations contribute to the peaks centred at about 2900 cm^{-1} -2600 cm^{-1} [41]. The broad peaks at around 1650 cm^{-1} -1590 cm^{-1} are assigned to the N–H deformation of the amine group [41, 42]. This confirms that amino groups have been grafted into CNTs. The nanocomposite membrane clearly exhibited a broad peak at a wave number of 3480 cm^{-1} which corresponds with the presence of bound water and the -OH functional group on the surface of the Zr nanoparticles as shown in Fig. 7d(a). Due to the water that tightly bound on the surface of the Zr nanoparticles, it is highly stable at a temperature higher than 100 °C. Fig. 7d(a) shows the vibration peak at 1016 cm^{-1} that could be attributed to the vibrational mode of Zr–O and the peak at 1550 cm^{-1} that could be due to Zr–OH bending vibrations, indicating the presence of zirconia nanoparticles within the modified Nafion® membrane [43]. Fig. 7d(b) shows the O–H vibration of physically adsorbed water occurring at wave numbers of 3451 cm^{-1} and 3456 cm^{-1} [44]. Fig. 7d(b) shows the vibration peaks at 1195 cm^{-1} and 1198 cm^{-1} that attributed to the $-CF_2-CF_2-$ vibration, and 1060 cm^{-1} attributed to $-SO_3^-$ [45].

3.4. Contact angle, water uptake, swelling ratio, ion exchange capacity and proton conductivity measurement

The contact angle was measured to determine the effect of ZrO_2-CNT nanoparticles in hydrophilicity and hydrophobicity of modified Nafion® membranes. The digital images of water droplets at the surface area of commercial and modified membrane are presented in Fig. 8. Fig. 8 shows that commercial Nafion® 117 membranes are hydrophobic surfaces since they have obtained the contact angle above 90°, whereas the modified Nafion® membrane with ZrO_2-CNT nanoparticles acts as a hydrophilic surface as the obtained contact angles are less than 90°. Generally, the contact angles of the modified membranes were decreasing when compared with that of unmodified Nafion® 117 membranes. This was due to the hydrophilicity of ZrO_2-CNT nanoparticles that enhancing the hydrophilicity of the membrane. The contact angles obtained show no differences when recorded on 10 test. Contact angles below 90° indicate the hydrophilic character of a sample, describing the water-uptake capability. In Fig. 8(b) it was observed that when the water droplet touched the commercial Nafion® 117 membrane, it immediately swells within the measuring time [46]. This may be due to the hydrophobic groups on the backbones and hydrophilic groups on the sulfonate heads of Nafion® membranes [46]. The water uptake of Nafion®/ZrO_2-CNT nanocomposite membranes and Nafion® 117 membranes was obtained by soaking the membranes in water at room temperature for 24 hours. Nafion®/ZrO_2-CNT nanocomposite membranes obtain a higher water uptake of 52%, than the commercial Nafion® 117 membranes (30%) as shown in Table 1. The results show that the incorporation of ZrO_2-CNT nanoparticles increases the water uptake of the Nafion® 117 membranes due to inorganic nanoparticles that enhanced the hydrogen bonding sites. The dimensional swelling ratio of Nafion®/ZrO_2-CNT nanocomposite membranes (16.7%) is slightly higher than commercial Nafion® 117

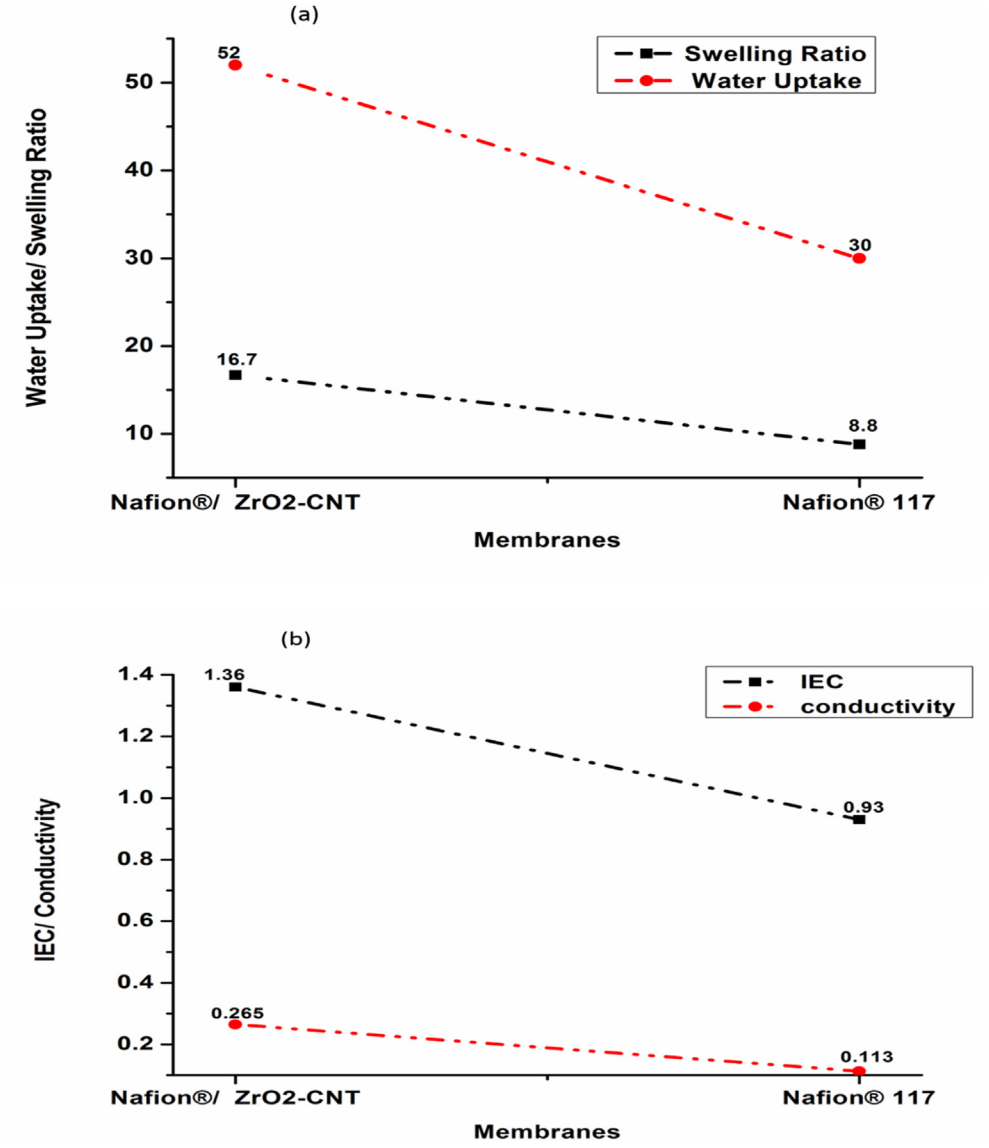

Fig. 9. (a) Water uptake and swelling ratio, (b) Ion exchange capacity and proton conductivity measurement of Nafion®/ZrO_2-CNT nanocomposite membranes and Nafion® 117 membrane.

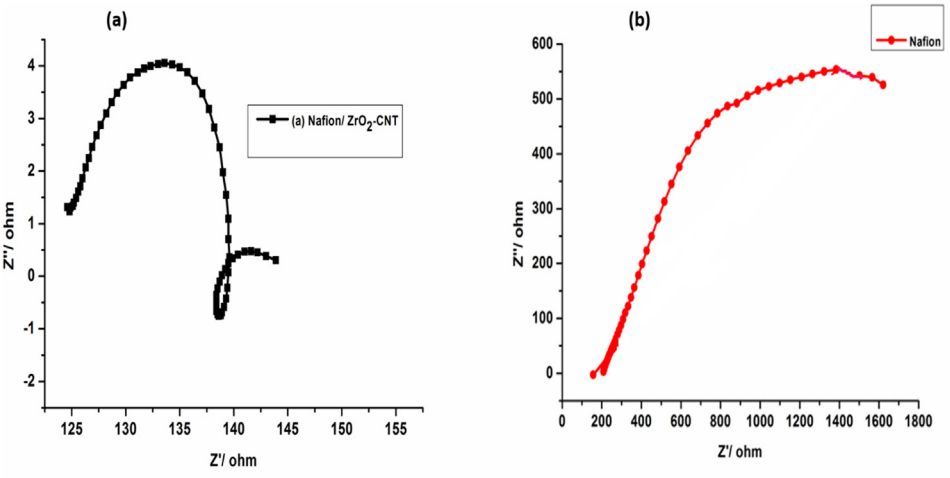

Fig. 10. Complex-plane of imaginary impendance (-Z") versus real impendance (Z') of (a) Nafion®/ZrO_2-CNT nanocomposite membrane and (b) Nafion® 117 membrane.

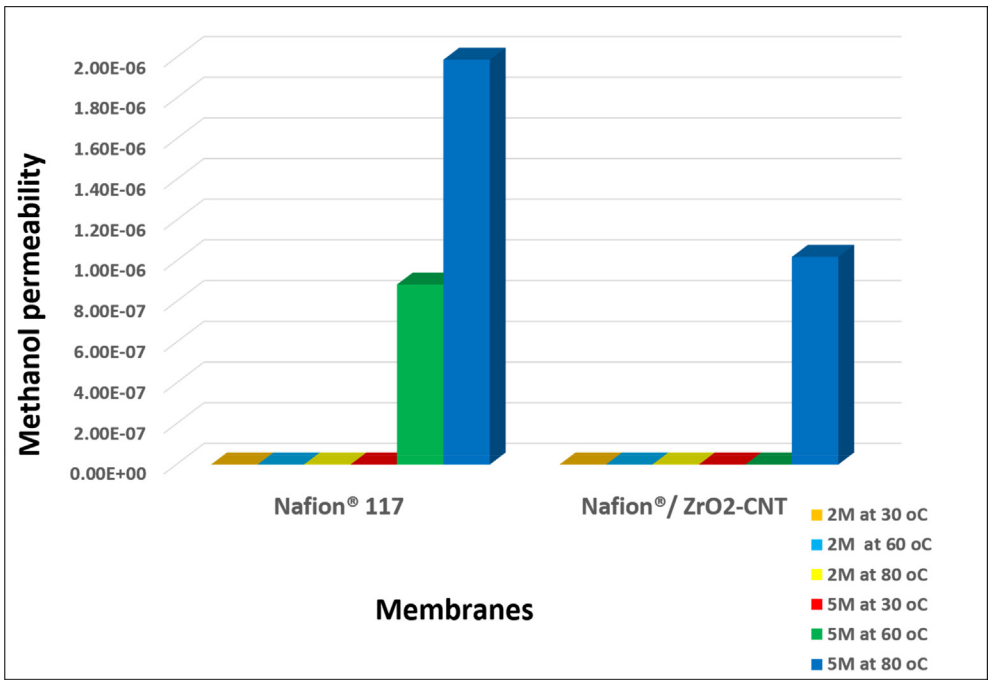

Fig. 11. Comparison of methanol crossover (5 M and 2 M concentration) of Nafion® 117 membrane and Nafion®/ZrO_2-CNT nanocomposite membrane at 30 °C, 60 °C and 80 °C.

membrane (8.8%), this is due to the absorbed water within the membrane matrix as shown in Table 1 and Fig. 9. Table 1 and Fig. 9 shows that nanocomposites membrane obtained a higher IEC value of 1.36 meg. g^{-1} when compared to 0.93 meg. g^{-1} of commercial Nafion® 117 membrane. These high IEC value may due to the incorporation of ZrO_2-CNT nanoparticles, which increased the membrane acid property for providing new strong acid site. The conductivity of all the membranes were presented in Fig. 9 and Table 1. The results shows that the proton conductivity of Nafion®/ZrO_2-CNT nanocomposite membrane and Nafion® 117 membrane were 0.113 S/cm and 0.265 S/cm, respectively. These higher conductivity may due to the incorporation of CNT which is higher in ionic conductivity and ZrO_2 nanoparticles which retain water within the membranes [47]. Fig. 10 shows the Nyquist plot of Nafion®/ZrO_2-CNT nanocomposite membrane and Nafion® 117 membrane. The results show that Nafion®/ZrO_2-CNT nanocomposite membrane obtained lower resistance than Nafion® 117 membrane as shown in Fig. 10(a & b). Furthermore, the lower resistance is due to the incorporation of nanoparticles that enhance the conductivity, which will showed the good performance for fuel cell.

3.5. *Methanol permeability*

The methanol permeability of membranes were measured under 2 M and 5 M methanol solution at 30 °C, 60 °C and 80 °C. At the lower temperature of 30 °C and 60 °C they were no methanol crossover through the nanocomposite membranes (0 cm^2/s) as shown in Fig. 11 [48]. Whereas for commercial Nafion® 117 membrane at 5 M and 60 °C shows the methanol permeation of 8.84×10^{-7} cm^2/s [49] which is higher than modified membrane. This may be due to ZrO_2-CNT nanoparticles that incoprated within the Nafion membrane, which blocked the methanol permeation. Furthermore, this methanol reduction makes this electrolytes suitable used in DMFC applications. At the higher temperature of 80 °C and higher methanol concentration of 5 M, the methanol permeation of commercial Nafion® 117 rise to 1.99×10^{-6} cm^2/s which double the value of Nafion®/ZrO_2-CNT nanocomposite membranes (1.02×10^{-6} cm^2/s), this may be due to ZrO_2-CNT nanoparticles that decreases the methanol crossover within Nafion® membrane.

4. Conclusion

The mechanical properties of Nafion® 117 membrane were improved by using ZrO_2-CNT nanoparticles as an inorganic filler. The effects of ZrO_2-CNT nanoparticles on the structure, morphology, hydrophilicity, thermal and mechanical stability of modified Nafion® membrane were observed under tensile testing, water contact angle content, XRD, TGA, SEM and AFM. The incorporation of ZrO_2-CNT nanoparticles into a Nafion® matrix has improved its hydrophilicity, as there is an improvement in the swelling of modified membrane when in contact with water. It was observed that the addition of ZrO_2-CNT nanoparticles increased the water content of the modified membrane that makes good electrolytes suitable to be used in fuel cells at high temperature and low relative humidity. XRD results show that ZrO_2-CNT nanoparticles have an impact on the crystallinity of modified Nafion® membrane when compared to the Nafion® 117 membrane. TGA of modified Nafion® membrane was found to have more thermal stability when compared with Nafion® 117 membrane that was totally burnt. The Nafion®/ZrO_2-CNT nanocomposite membrane obtained lower resistance with the decreased in methanol crossover than Nafion® 117 membrane, which shows a potential in direct fuel cells. In conclusion, the water uptake, swelling ratio, IEC and proton conductivity of nanocomposite membranes was higher than commercial Nafion® 117 membrane. That shows the improvement of modified Nafion® membrane, which makes them suitable used in fuel cell application.

Declarations

Author contribution statement

Rudzani Sigwadi: Conceived and designed the experiments; Performed the experiments; Analyzed and interpreted the data; Wrote the paper.

Touhami Mokrani: Performed the experiments.

Mokhotjwa Simon Dhlamini: Analyzed and interpreted the data.

Fulufhelo Nemavhola: Performed the experiments; Contributed reagents, materials, analysis tools or data.

Funding statement

This work was supported by the National Research Funding (NRF) and the University of South Africa (AQIP).

Competing interest statement

The authors declare no conflict of interest.

Additional information

No additional information is available for this paper.

References

[1] K. Ketpang, et al., Porous zirconium oxide nanotube modified Nafion composite membrane for polymer electrolyte membrane fuel cells operated under dry conditions, J. Membr. Sci. 488 (2015) 154–165.
[2] A. Hagfeldt, et al., Dye-sensitized solar cells, Chem. Rev. 110 (11) (2010) 6595–6663.
[3] A. Sacca, et al., Nafion–TiO 2 hybrid membranes for medium temperature polymer electrolyte fuel cells (PEFCs), J. Power Sources 152 (2005) 16–21.
[4] M. Mazaheri, et al., Multi-walled carbon nanotube/nanostructured zirconia composites: outstanding mechanical properties in a wide range of temperature, Compos. Sci. Technol. 71 (7) (2011) 939–945.
[5] Jiménez, K.A.R., et al., Nav View Search.
[6] A. Duszová, et al., Microstructure and properties of carbon nanotube/zirconia composite, J. Eur. Ceram. Soc. 28 (5) (2008) 1023–1027.
[7] C.R. Babu, N.R.M. Reddy, K. Reddy, Synthesis and characterization of high dielectric nano zirconium oxide, Ceram. Int. 41 (9) (2015) 10675–10679.
[8] İ. Uslu, et al., Synthesis and characterization of boron doped alumina stabilized zirconia fibers, Fibers Polym. 12 (3) (2011) 303–309.
[9] C. Guo, et al., Synthesis and characterization of ZrO 2 hollow spheres, Mater. Lett. 63 (12) (2009) 1013–1015.
[10] Y.-F. Zhu, et al., Synthesis of zirconia nanoparticles on carbon nanotubes and their potential for enhancing the fracture toughness of alumina ceramics, Compos. B Eng. 39 (7) (2008) 1136–1141.
[11] H. Huo, et al., Chiral zirconia nanotubes prepared through a sol–gel transcription approach, J. Mater. Chem. 2 (2) (2014) 333–338.
[12] D.J. Kim, M.J. Jo, S.Y. Nam, A review of polymer–nanocomposite electrolyte membranes for fuel cell application, J. Ind. Eng. Chem. 21 (2015) 36–52.
[13] H. Wang, et al., Synthesis of 3D graphite oxide-exfoliated carbon nanotube carbon composite and its application as catalyst support for fuel cells, J. Power Sources 260 (2014) 338–348.
[14] J. Shi, et al., Graphene reinforced carbon nanotube networks for wearable strain sensors, Adv. Funct. Mater. 26 (13) (2016) 2078–2084.
[15] M. Dresselhaus, et al., Electronic, thermal and mechanical properties of carbon nanotubes, Phil. Trans. R. Soc. Lond. A: Math. Phys. Eng. Sci. 362 (1823) (2004) 2065–2098.
[16] C. Lu, Y.-W. Mai, Anomalous electrical conductivity and percolation in carbon nanotube composites, J. Mater. Sci. 43 (17) (2008) 6012–6015.
[17] V. Gupta, N. Miura, Polyaniline/single-wall carbon nanotube (PANI/SWCNT) composites for high performance supercapacitors, Electrochim. Acta 52 (4) (2006) 1721–1726.
[18] M. Hughes, et al., Electrochemical capacitance of a nanoporous composite of carbon nanotubes and polypyrrole, Chem. Mater. 14 (4) (2002) 1610–1613.
[19] K.H. An, et al., Supercapacitors using singlewalled carbon nanotube electrodes, in: AIP Conference Proceedings, AIP, 2001.
[20] E. Frackowiak, Carbon materials for supercapacitor application, Phys. Chem. Chem. Phys. 9 (15) (2007) 1774–1785.
[21] B. Bae, H.Y. Ha, D. Kim, Nafion®-graft-polystyrene sulfonic acid membranes for direct methanol fuel cells, J. Membr. Sci. 276 (1) (2006) 51–58.
[22] J.-M. Thomassin, et al., Beneficial effect of carbon nanotubes on the performances of Nafion membranes in fuel cell applications, J. Membr. Sci. 303 (1) (2007) 252–257.
[23] R. Sigwadi, et al., Effect of synthesis temperature on particles size and morphology of zirconium oxide nanoparticle, J. Nano Res. (2017). Trans Tech Publ.
[24] R. Manivannan, et al., Thermal stability of zirconia-coated multiwalled carbon nanotubes, Def. Sci. J. 60 (3) (2010) 337.
[25] C.,S.S. Yang, A.B. Bocarsly, S. Tulyani, J.B. Benziger, A comparison of physical properties and fuel cell performance of Nafion and zirconium phosphate/Nafion composite membranes, J. Membr. Sci. 237 (1-2) (2004) 145–161.
[26] G. Vaivars, et al., Zirconium phosphate based inorganic direct methanol fuel cell, Mater. Sci. 10 (2004) 162–165.
[27] P. Khalid, et al., Synthesis and characterization of carbon nanotubes reinforced hydroxyapatite composite, Indian J.Sci.Technol. 6 (12) (2013) 5546–5551.
[28] H. Yu, et al., Hydrophilicity and hydrophobicity study of catalyst layers in proton exchange membrane fuel cells, Electrochim. Acta 51 (7) (2006) 1199–1207.
[29] L. Wu, et al., Environmentally friendly synthesis of alkaline anion exchange membrane for fuel cells via a solvent-free strategy, J. Membr. Sci. 371 (1) (2011) 155–162.
[30] W. Zhengbang, H. Tang, P. Mu, Self-assembly of durable Nafion/TiO 2 nanowire electrolyte membranes for elevated-temperature PEM fuel cells, J. Membr. Sci. 369 (1) (2011) 250–257.
[31] P. Velayutham, A.K. Sahu, S. Parthasarathy, A nafion-ceria composite membrane electrolyte for reduced methanol crossover in direct methanol fuel cells, Energies 10 (2) (2017) 259.
[32] J. Suntivich, et al., A perovskite oxide optimized for oxygen evolution catalysis from molecular orbital principles, Science 334 (6061) (2011) 1383–1385.
[33] P. James, et al., Hydration of Nafion® studied by AFM and X-ray scattering, J. Mater. Sci. 35 (20) (2000) 5111–5119.
[34] M. Nagai, K. Kobayashi, Y. Nakajima, Inorganic–orgnic composite protonic conductors comprising silicophosphate glass and ion-exchange resin, Solid State Ion. 136 (2000) 249–254.
[35] Z.-G. Shao, P. Joghee, I.-M. Hsing, Preparation and characterization of hybrid Nafion–silica membrane doped with phosphotungstic acid for high temperature operation of proton exchange membrane fuel cells, J. Membr. Sci. 229 (1-2) (2004) 43–51.
[36] M. Osińska, et al., Study of the role of ceramic filler in composite gel electrolytes based on microporous polymer membranes, J. Membr. Sci. 326 (2) (2009) 582–588.
[37] K.T. Adjemian, et al., Function and characterization of metal oxide– nafion composite membranes for elevated-temperature H2/O2 PEM fuel cells, Chem. Mater. 18 (9) (2006) 2238–2248.
[38] M. Jansen, E. Guenther, Oxide gels and ceramics prepared by a nonhydrolytic sol-gel process, Chem. Mater. 7 (11) (1995) 2110–2114.
[39] Y. Hao, et al., Preparation of ZrO2–Al2O3 composite membranes by sol–gel process and their characterization, Mater. Sci. Eng. A 367 (1-2) (2004) 243–247.
[40] A.C. Fernandes, E.A. Ticianelli, A performance and degradation study of Nafion 212 membrane for proton exchange membrane fuel cells, J. Power Sources 193 (2) (2009) 547–554.
[41] V. Di Noto, et al., Effect of SiO2 on relaxation phenomena and mechanism of ion conductivity of [Nafion/(SiO2) x] composite membranes, J. Phys. Chem. B 110 (49) (2006) 24972–24986.
[42] M. Ludvigsson, J. Lindgren, J. Tegenfeldt, FTIR study of water in cast Nafion films, Electrochim. Acta 45 (14) (2000) 2267–2271.
[43] D. Sarkar, et al., Synthesis and characterization of sol–gel derived ZrO 2 doped Al 2 O 3 nanopowder, Ceram. Int. 33 (7) (2007) 1275–1282.
[44] H. Yang, et al., Preparation of Nafion/various Pt-containing SiO2 composite membranes sulfonated via different sources of sulfonic group and their application in self-humidifying PEMFC, J. Membr. Sci. 443 (2013) 210–218.
[45] Y. Zhai, et al., Preparation and characterization of sulfated zirconia (SO42−/ZrO2)/Nafion composite membranes for PEMFC operation at high temperature/low humidity, J. Membr. Sci. 280 (1-2) (2006) 148–155.
[46] L. Zou, et al., Surface hydrophilic modification of RO membranes by plasma polymerization for low organic fouling, J. Membr. Sci. 369 (1-2) (2011) 420–428.
[47] K. Li, et al., Self-assembled Nafion®/metal oxide nanoparticles hybrid proton exchange membranes, J. Membr. Sci. 347 (1-2) (2010) 26–31.
[48] Y. Hudiono, et al., Porous layered oxide/Nafion® nanocomposite membranes for direct methanol fuel cell applications, Microporous Mesoporous Mater. 118 (1-3) (2009) 427–434.
[49] R. Sigwadi, et al., The impact of zirconia nano-rods on the methanol permeability and conductivity of Nafion®-ZrO2 nano-composite membrane, Int. J. Microstruct. Mater. Prop. 13 (6) (2018) 381–402.